SUPPLEMENTAL INFORMATION

Figure S1 (corresponding to Fig. 1)

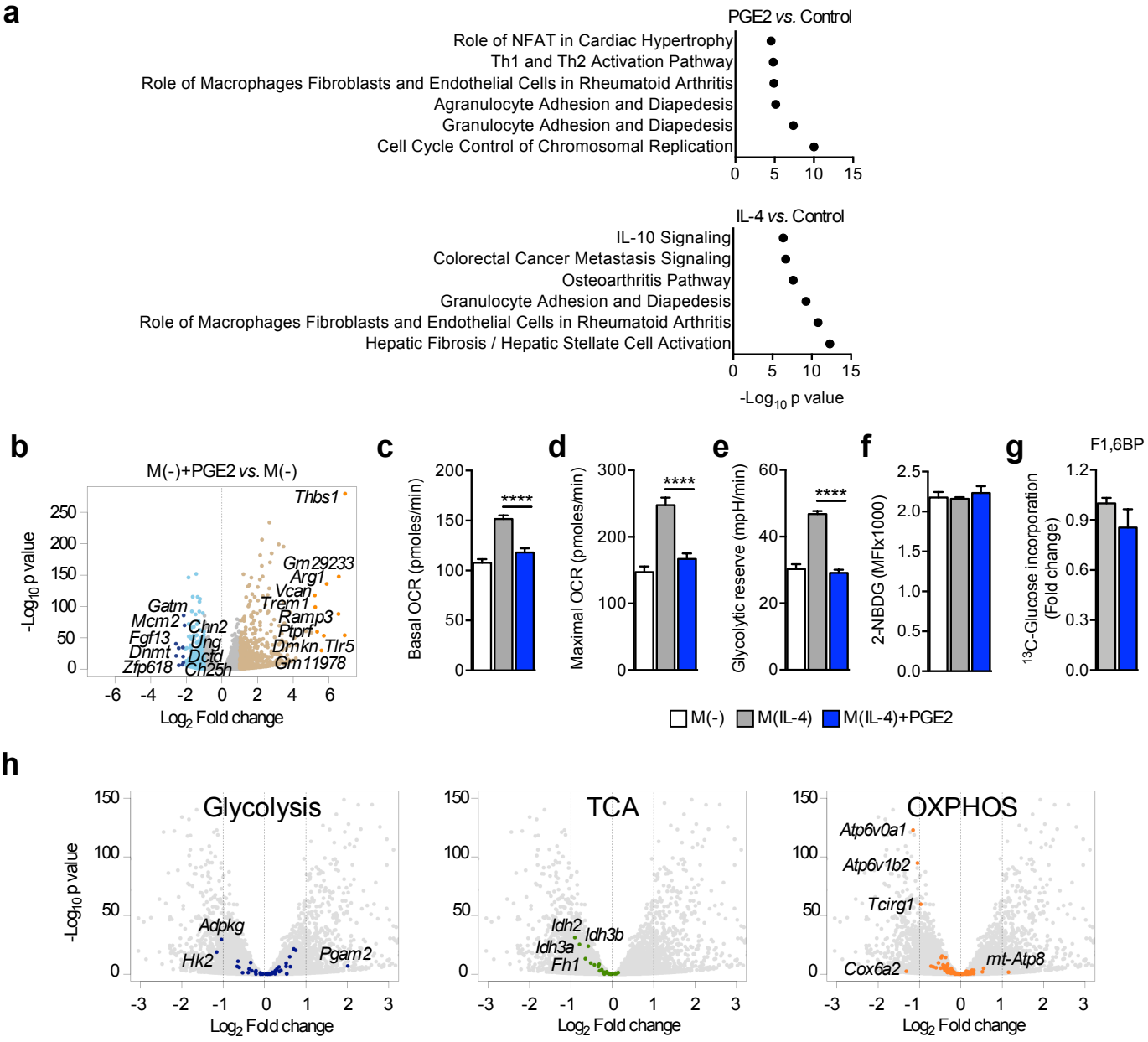

Supplemental figure 1 (corresponding to figure 1). PGE2 modifies macrophage activation and metabolism.

(a) Canonical pathways enriched in M(-)+PGE2 (top) or M(IL-4) (bottom) cells compared to M(-) determined using Ingenuity Pathway Analysis of RNA-seq data. **(b)** Volcano plot showing top 10 up (dark orange) and down (dark blue) regulated genes in M(-)+PGE2 cells compared to M(-). Measurements of **(c)** OCR, **(d)** maximal respiration, **(e)** glycolytic reserve, and **(f)** uptake of 0.1 µg/ml 2-NBDG in M(-), M(IL-4) and M(IL-4)+PGE2 treated BMMs after 24 h. Data are representative of 3 independent experiments. Bars are mean ± SEM from 4-6 biological replicates (p****<0.0001). **(g)** Phosphofructokinase activity was indirectly assessed by measuring the incorporation of ^{13}C-Glucose into fructose-1,6-biphosphate (F1,6BP) via LC-MS from cells stimulated for 24 h with indicated treatments. Bars represent mean ± SEM from 3 biological replicates normalized to M(IL-4). **(h)** Volcano plots of differentially expressed genes in M(IL-4)+PGE2 cells treated for 6 h compared to M(IL-4), highlighting key metabolic pathways obtained from the Kyoto Encyclopedia of genes and genomes (pathway identifiers: Glycolysis – 00010; TCA – 00020; OXPHOS – 00190).

Figure S2 (corresponding to Fig. 2)

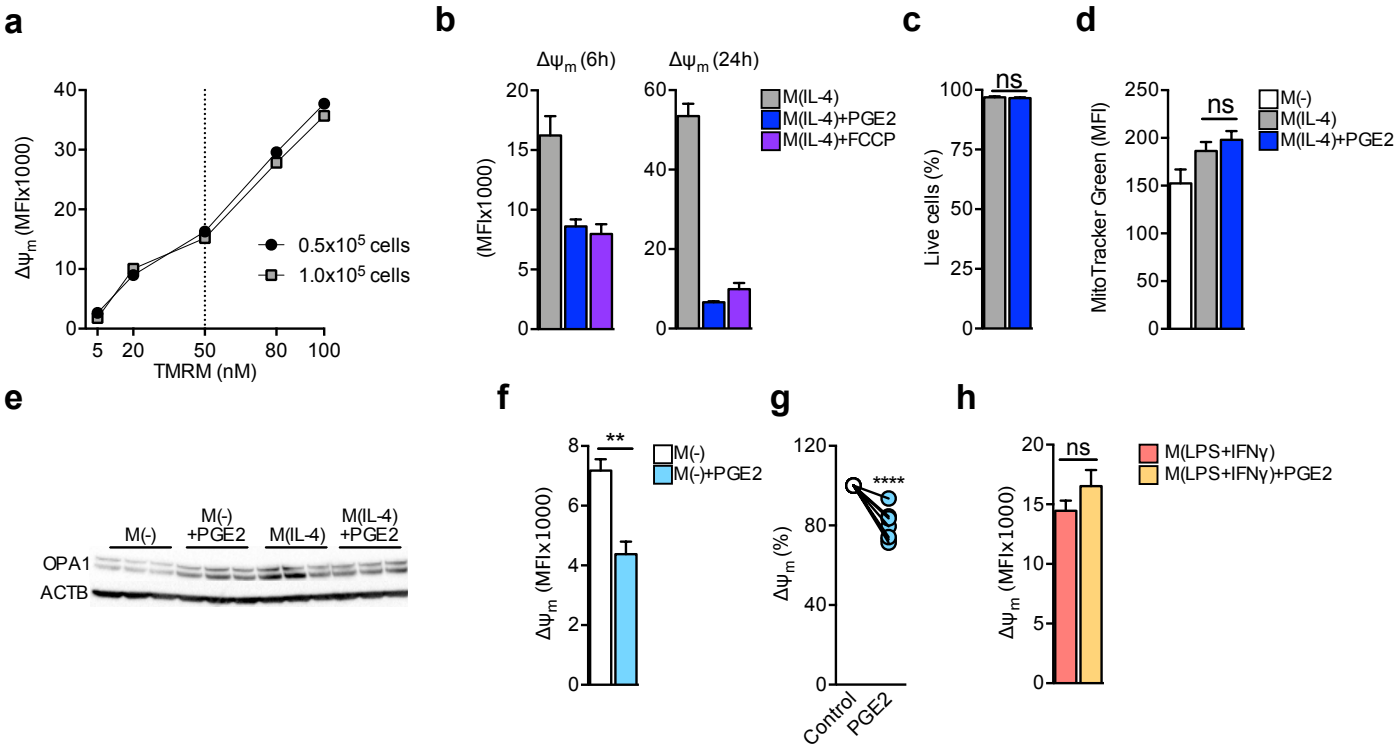

Supplemental figure 2 (corresponding to figure 2). Regulation of $\Delta\psi_m$ by PGE2 is not linked to a loss of cell viability, reduced mitochondrial mass or increased mitochondrial fission, requires robust respiration, and is conserved across macrophages from different sources.

Flow cytometric analysis of **(a)** linearity of TMRM doses across different cell numbers, **(b)** effects of 15μM FCCP on $\Delta\psi_m$ measured by TMRM, **(c)** the percentage of live cells and **(d)** MitoTracker Green incorporation in M(-), M(IL-4) and M(IL-4)+PGE2 BMMs after 6 h or 24 h culture. **(e)** Immunoblot analysis of OPA1 in M(-), M(-)+PGE2, M(IL-4) and M(IL-4)+PGE2 cells after 24 h of culture. Data are representative of 2 independent experiments. **(f-h)** Analysis of $\Delta\psi_m$ via incorporation of TMRM into **(f)** M(-) and M(-)+PGE2 cells, **(g)** control plus PGE2 treated human monocytes and **(h)** M(LPS+IFNγ) and M(LPS+IFNγ)+PGE2 BMMs, all after 24 h of culture. **(b-d, f-g)** Data are representative of 3 independent experiments. Bars are mean ± SEM from 3-6 biological replicates ($p^{**}<0.005$, $p^{****}<0.0001$). Symbols represent individual human subjects (paired T-test, $p^{****}<0.0001$).

Figure S3 (corresponding to Fig. 3)

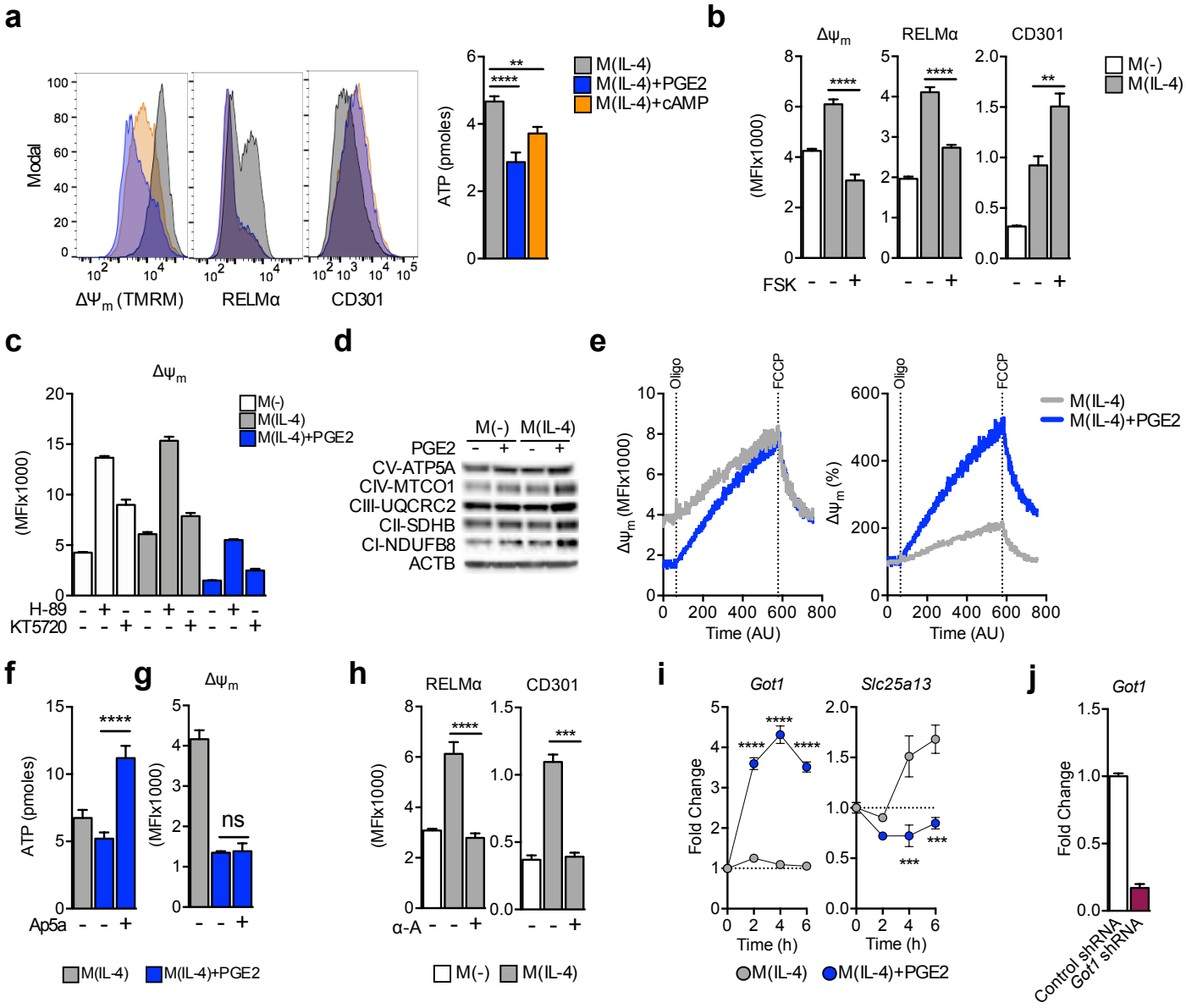

Supplemental figure 3 (corresponding to figure 3). PGE2 regulates membrane potential through cAMP and mitochondrial redox shuttles.

(a-b) Analysis of $\Delta\psi_m$, RELMα and CD301 via flow cytometry, **(a)** and ATP concentration via colorimetric assay, of **(a)** M(IL-4), M(IL-4)+PGE2 and IL-4 stimulated BMMs treated with 100 μM 8-Br-cAMP (M(IL-4)+cAMP), or **(b)** M(-), and M(IL-4) cells treated with 20 μM Forskolin (FSK) after 24 h of culture. Data are representative of 3 independent experiments. Bars are mean ± SEM from 3-4 biological replicates (p**<0.005, p****<0.0001). Representative histograms are shown. **(c)** Flow cytometric analysis of $\Delta\psi_m$ measured by TMRM in M(-), M(IL-4) and M(IL-4)+PGE2 cells after 24 h of culture treated with PKA inhibitors 10 μM H-89 or 10 μM KT5720. **(d)** Immunoblot analysis of electron transport chain complexes in BMMs treated as indicated for 24 h. Data are representative of 2 independent experiments. **(e)** Real time measurement of $\Delta\psi_m$ assayed via flow cytometry by incorporation of TMRM in M(IL-4) or M(IL-4)+PGE2 cells in response to 1 μM oligomycin followed by 15 μM FCCP. **(f)** Analysis of $\Delta\psi_m$ via flow cytometry, **(g)** and ATP concentration via colorimetric assay of M(IL-4) and M(IL-4)+PGE2 cells treated as indicated with 100 μM Ap5a after 24 h of culture. Data are representative of 3 independent experiments. Bars are mean ± SEM from 5-8 biological replicates (p****<0.0001). **(h)** Analysis of RELMα and CD301 via flow cytometry of BMMs treated as indicated in the presence or absence of 2 μg/ml α-amanitin (α-A), all after 24 h of culture. Data are representative of 3 independent experiments. Bars are mean ± SEM from 6 biological replicates (p***<0.0005, p****<0.0001). **(i)** mRNA obtained from indicated times post stimulation was tested by qRT-PCR to determine expression of *Got1* and *Slc25a13* in M(IL-4) and M(IL-4)+PGE2 cells normalized to 0 h time point. Symbols are mean ± SEM from 4 biological replicates (p***<0.0005, p****<0.0001). **(j)** Validation of *Got1* knock down with targeted shRNA. Data are representative of 2 independent experiments.

Figure S4 (corresponding to Fig. 4)

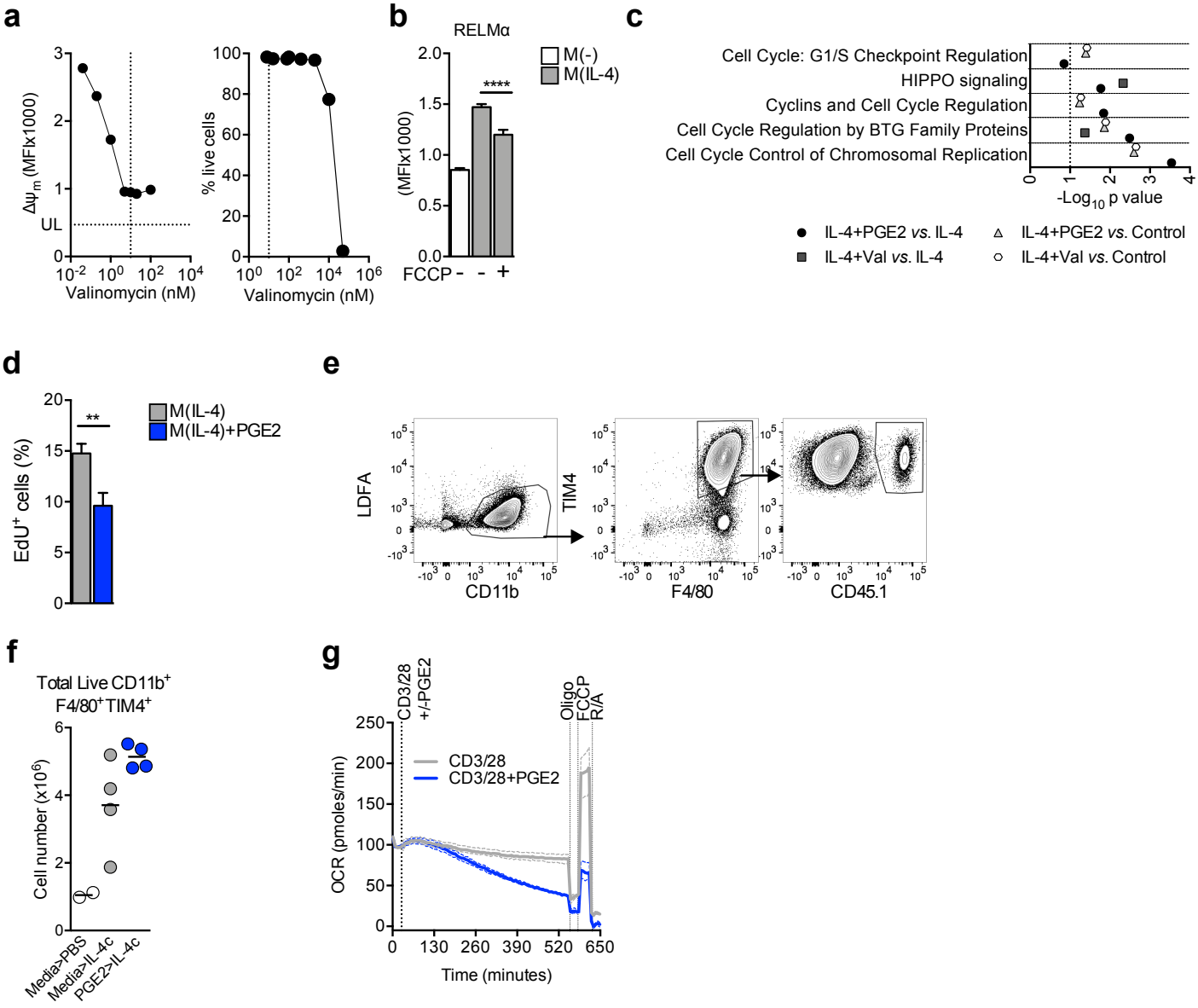

Supplemental figure 4 (corresponding to figure 4). Mitochondrial membrane potential regulates gene expression and cell cycle.

(a) Analysis of acute effects on $\Delta\psi_m$, and over night effects on viability of several doses of Val. Data are representative of 2 independent experiments. **(b)** Analysis of RELMα expression via flow cytometry in cells treated with IL-4 for 24 h in the presence or absence of 1.5 μM FCCP after 4 hours of initial stimulation. Data are representative of 2 independent experiments. Bars are mean ± SEM from 4 biological replicates (p****<0.0001). **(c)** Enriched canonical pathways determined by Ingenuity Pathway Analysis based on expression of VRGs from M(IL-4)+PGE2 and M(IL-4)+Val cells compared to M(-) or M(IL-4). **(d)** EdU incorporation into M(IL-4) and M(IL-4)+PGE2 cells after 24 h of treatment. Data are representative of 3 independent experiments. Bars are mean ± SEM from 6 biological replicates (p**<0.005). **(e)** Gating strategy for CD45.1 pMacs stimulated *ex vivo* with PGE2, then adoptively transferred into the peritoneum of CD45.2 mice. Representative contour plots shown. **(f)** Absolute number of live $CD11b^+F4/80^+TIM4^+$ cells. Data are representative of 3 independent experiments. Symbols represent biological replicates. **(g)** $CD8^+$ T cells were activated with CD3+CD28 in the presence or absence of PGE2, and then EFA activation profile was recorded over a period of 11 h. Data are representative of 2 independent experiments.

Figure S5 (corresponding to Fig. 5)

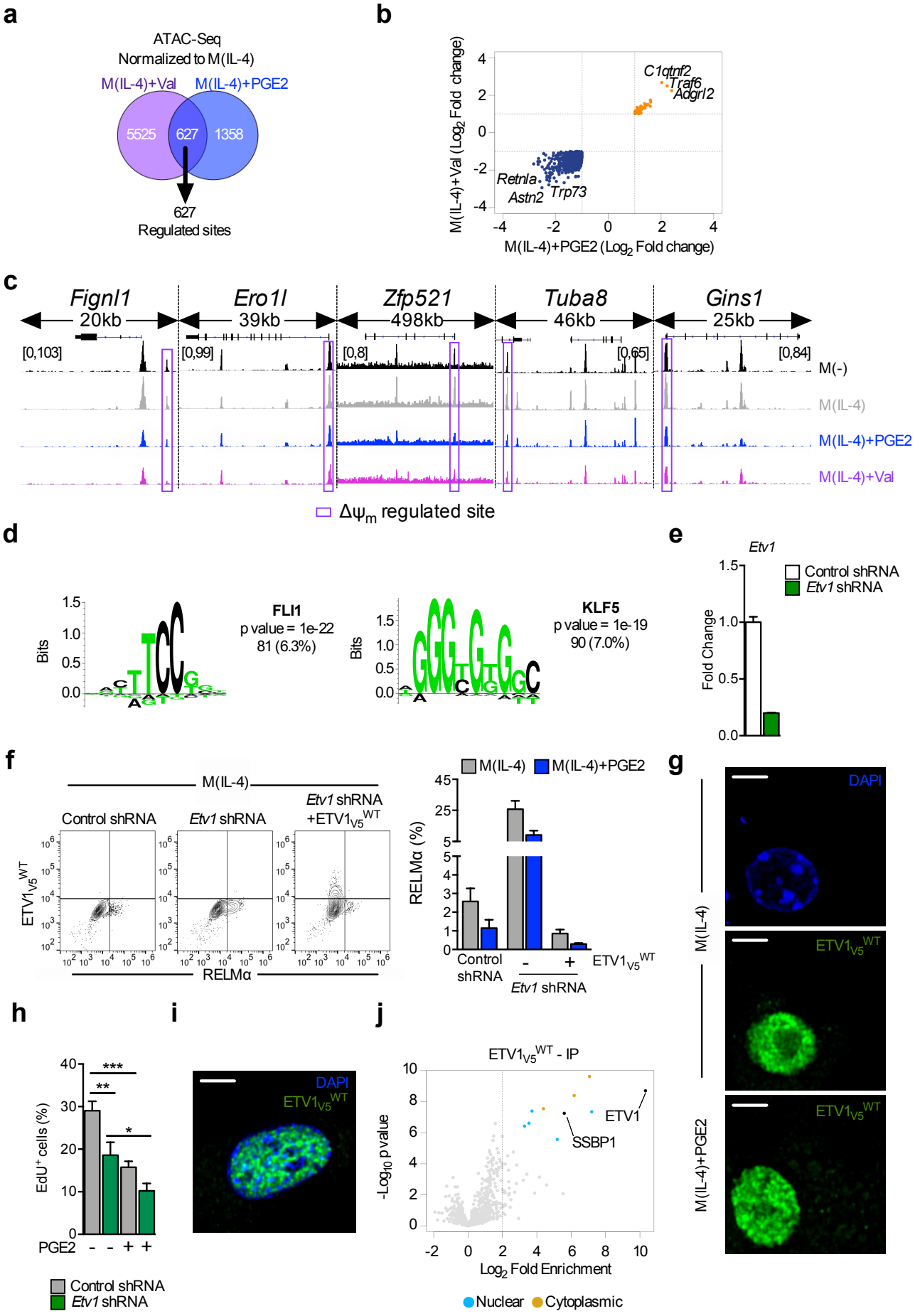

Supplemental figure 5 (corresponding to figure 5). ETV1 is a mitochondrial membrane potential regulated transcription factor.

(a) Venn diagram showing sites in the chromatin with coincident increased or decreased accessibility in M(IL-4)+PGE2 and M(IL-4)+Val cells compared to M(IL-4) after 6 h of stimulation. **(b)** Fold change in accessibility of 627 regions with coincident regulation by PGE2 and Val. Representative genes with less accessible regions (blue) as well as those with increased accessibility (orange) are shown. **(c)** Regions of accessible chromatin, as determined by ATAC-seq, in the loci of VRGs from cells treated as indicated for 6 h. $\Delta\psi_m$-regulated peaks (purple solid lines) are highlighted. **(d)** Second and third most enriched transcription factor motifs from regulatory regions of promoters (up to 20kb upstream from TSS) of VRGs with reported p values and number plus percentage of matching regulatory regions out of 1286 detected. **(e)** Validation of *Etv1* knock down with targeted shRNA. Data are representative of 2 independent experiments. **(f-h)** BMMs were transduced with a control or an *Etv1*-shRNA. **(f-g)** *Etv1*-shRNA transduced cells were simultaneously engineered to express a V5 tagged variant of ETV1. **(f)** Analysis of RELMα and V5 tagged ETV1 expression via flow cytometry was carried out in M(IL-4) and M(IL-4)+PGE2 cells after 24 h of culture. Representative contour plots are shown. Bars are mean ± SEM from 3 biological replicates and are representative of 3 independent experiments. **(g)** M(IL-4) and M(IL-4)+PGE2 cells treated for 6 h were labeled with an anti-V5 antibody, counter stained with DAPI and imaged using confocal microscopy. Images are representative of 3 biological replicates and 3 independent experiments. Scale bar = 5 μm. **(h)** EdU incorporation into transduced M(IL-4) and M(IL-4)+PGE2 cells after 24 h of treatment was examined. Bars are mean ± SEM from 6 biological replicates ($p^*<0.05$, $p^{**}<0.005$, $p^{***}<0.0005$). Data are representative of 2 independent experiments. **(i-j)** *Etv1*-shRNA transduced MEFs were simultaneously engineered to express a V5 tagged variant of ETV1. **(i)** MEFs were labeled with an anti-V5 antibody, counter stained with DAPI and imaged using confocal microscopy. Images are representative of 3 replicates and 2 independent experiments. Scale bar = 5 μm. **(j)** Volcano plot depicting proteins detected by mass spectrometry in IP pull downs with anti-V5 antibody in MEF cell lysates expressing V5-tagged ETV1. Significantly enriched proteins (lower than 1% FDR and greater than 4 fold enrichment) are highlighted. Data was generated from 3 replicates. Enrichment was calculated over negative IP controls.